Bone marrow-derived mononuclear cell seeded bioresorbable vascular graft improves acute graft patency by inhibiting thrombus formation via platelet adhesion☆

Hideki Miyachi [a,b], James W. Reinhardt [a], Satoru Otsuru [c], Shuhei Tara [a,b], Hidetaka Nakayama [d], Tai Yi [a], Yong-Ung Lee [a], Shinka Miyamoto [a], Toshihiro Shoji [a], Tadahisa Sugiura [a], Christopher K. Breuer [a], Toshiharu Shinoka [a,e,*]

[a] Tissue Engineering Program and Center for Cardiovascular and Pulmonary Research, The Research Institute at Nationwide Children's Hospital, Columbus, OH, USA
[b] Department of Cardiovascular Medicine, Nippon Medical School, Tokyo, Japan
[c] Center for Childhood Cancer and Blood Disease, The Research Institute at Nationwide Children's Hospital, Columbus, OH, USA
[d] QOL Research Center Laboratory, Gunze Limited, Ayabe-Shi, Kyoto, Japan
[e] Department of Cardiothoracic Surgery, The Heart Center, Nationwide Children's Hospital, Columbus, OH, USA

ARTICLE INFO

ABSTRACT

Background: Acute thrombosis is a crucial cause of bioresorbable vascular graft (BVG) failure. Bone marrow-derived mononuclear cell (BM-MNC)-seeded BVGs demonstrated high graft patency, however, the effect of seeded BM-MNCs against thrombosis remains to be elucidated. Thus, we evaluated an antithrombotic effect of BM-MNC-seeding and utilized platelet-depletion mouse models to evaluate the contribution of platelets to acute thrombosis of BVGs.

Methods and results: BVGs were composed of poly(glycolic acid) mesh sealed with poly(ʟ-lactideco-ε-caprolactone). BM-MNC-seeded BVGs and unseeded BVGs were implanted to wild type C57BL/6 mice (n = 10/group) as inferior vena cava interposition conduits. To evaluate platelet effect on acute thrombosis, c-Mpl$^{-/-}$ mice and Pf4-Cre^{+}; iDTR mice with decreased platelet number were also implanted with unseeded BVGs (n = 10/group). BVG patency was evaluated at 2, 4, and 8 weeks by ultrasound. BM-MNC-seeded BVGs demonstrated a significantly higher patency rate than unseeded BVGs during the acute phase (2-week, 90% vs 30%, p = .020), and patency rates of these grafts were sustained until week 8. Similar to BM-MNC-seeded BVGs, C-Mpl$^{-/-}$ and Pf4-Cre^{+}; iDTR mice also showed favorable graft patency (2-week, 90% and 80%, respectively) during the acute phase. However, the patency rate of Pf4-Cre^{+}; iDTR mice decreased gradually after DTR treatment as platelet number recovered to baseline. An in vitro study revealed BM-MNC-seeding significantly inhibited platelet adhesion to BVGs compared to unseeded BVGs, (1.75 ± 0.45 vs $8.69 \pm 0.68 \times 10^3$ platelets/mm^2, p < .001).

Conclusions: BM-MNC-seeding and the reduction in platelet number prevented BVG thrombosis and improved BVG patency, and those results might be caused by inhibiting platelet adhesion to the BVG.

1. Introduction

Vascular bypass and replacement surgeries are common and successful treatments for patients with cardiovascular disease. However, current synthetic grafts have limitations due to risk of thrombosis, stenosis, calcification, and the lack of growth capacity. Bioresorbable vascular grafts (BVGs) have emerged to address these limitations. In 2001, a first-in-human implantation of the pulmonary artery BVG seeded with endothelial cells cultured from the patient was reported [1]. Thereafter, a clinical trial implanting the BVGs seeded with bone marrow-derived mononuclear cells (BM-MNCs) into the venous circulation for extra total cavo-pulmonary connections has been performed in Japan and U.S., and favorable long-term results have been reported [2]. Although BM-MNC-seeding was applied to BVGs to promote vascular remodeling initially, it was also revealed that seeding BM-MNCs on BVGs improved the patency of the BVGs at both acute and chronic phases in mouse models [3–5]. However, the crucial mechanism for how BM-MNC-seeding prevents stenosis/occlusion of BVGs was still unclear.

We have previously shown that BVGs transform into functional mature blood vessels via an inflammation-mediated process of vascular remodeling, and BVG stenosis is driven excessive inflammation by infiltration of host monocytes and macrophage into BVG [4,5]. Although BM-MNC-seeding was shown to prevent chronic BVG stenosis by attenuating this inflammatory process [6], the role of BM-MNC-seeding in acute BVG stenosis, which is thought to be caused by acute thrombosis, has not been established. The purpose of the present study was to evaluate the antithrombotic effect of BM-MNC seeded BVGs in a mouse model and in vitro. Furthermore, platelet depletion models were utilized to evaluate the effect of platelets in BVG thrombosis on the basis of our previous report that platelets play a crucial role in BVG stenosis/occlusion during the early phase [6].

2. Materials and methods

2.1. Bioresorbable vascular grafts

All BVGs were provided by Gunze Ltd. (Kyoto, Japan). The BVGs were composed of nonwoven poly(glycolic acid) fiber mesh coated with a 50:50 copolymer sealant solution of poly(L-lactide-co-ε-caprolactone) (PLCL) as previously described [7]. Each graft was 3.0 mm in length with an inner diameter of 0.85 mm.

To seed BM-MNCs onto BVGs, syngeneic C57BL/6 mice were euthanized and bone marrow was collected from femurs and tibias with 5.0 ml of RPMI 1640 (Thermo Fisher scientific, Waltham, MA) and 1% penicillin/streptomycin (Sigma-Aldrich, St. Louis, MO). After filtration through a 70 μm cell strainer, the bone marrow was layered on Histopaque solution (1083, Sigma-Aldrich) in a 1:1 ratio (v/v). BM-MNCs were isolated using a density-gradient centrifugation method. A total of 1.0×10^6 cells suspended in 5 μl RPMI 1640 were seeded onto the scaffold for 10 min and then incubated overnight at 37 °C 5% CO_2 [8]. Cell concentrations were measured with Trypan blue exclusion using a Countess automated cell counter (Invitrogen, Carlsbad, CA).

2.2. Animal preparation

All animals received humane care in compliance with the National Institutes of Health Guideline for the Care and Use of Laboratory Animals. The Institutional Animal Care and Use Committee at Nationwide Children's Hospital approved the use of animal and all procedures described in this study. C57BL/6, C57BL/6-Tg(Pf4-cre)Q3Rsko/J (*Pf4-cre*), and C57BL/6-Gt(ROSA)26Sor$^{tm1(HBEGF)Awai}$/J (*iDTR*) mice were obtained from The Jackson Laboratories (Bar Harbor, ME). Homozygous c-Mpl–deficient ($c\text{-}mpl^{-/-}$) mice on a C57BL/6 background were obtained from Genentech (South San Francisco, CA). *Pf4-cre* mice were mated with the *iDTR* line to generate *Pf4-cre*; *iDTR* mice in our facilities. To induce megakaryocyte ablation in the *Pf4-cre*; *iDTR* model, diphtheria toxin (DT) (Sigma-Aldrich) was injected intraperitoneally every other day at a dose of 250 ng for two weeks after graft implantation.

2.3. Platelet number

To survey platelet number in C57BL/6, $c\text{-}Mpl^{-/-}$, and *Pf4-Cre*$^+$; *iDTR* mice, platelet numbers were counted using an ABX Micros 60 hematology analyzer (Horiba, Edison, NJ). Blood was collected from the retro orbital sinus of mice anesthetized with 1.5% v/v inhaled isoflurane by a capillary tube.

2.4. In vitro assessment of platelet attachment on BVGs

To measure platelet attachment on grafts, an LDH assay was performed as described before [9]. 0.6–1.2 ml of whole blood was obtained from a C57BL/6 mouse by intracardiac puncture with a 25 gauge needled affixed to 3 ml syringe preloaded with 100 μl of citrate-dextrose solution (C3821, Sigma-Aldrich). Platelet rich plasma (PRP) was prepared by centrifugation (120 g for 8 min ×2), and platelet number was counted by an ABX Micros 60 hematology analyzer. PRP was diluted with PBS to obtain a concentration of 0.2×10^6 cells/μl. BM-MNC-seeded BVGs and unseeded BVGs were incubated in PRP for 60 min at 37 °C, 5% CO_2 (n = 5, respectively). In addition, other BM-MNC-seeded BVGs were incubated into PBS for 60 min at 37 °C, 5% CO_2 (n = 5) as controls. Non-adherent platelets were removed by washing scaffolds with 1.0 ml of PBS. To lyse attached platelets, BVGs were soaked in 2% Triton X-100 (93,427, Sigma-Aldrich) for 60 min at room temperature, then an LDH assay was performed according to the manufacturer's instructions (MK401, Takara Bio, Kusatsu, Japan). Absorbance was measured at 490 nm using a SpectraMax M5 plate reader (Molecular Devices, Sunnyvale, CA), and a standard curve was applied to obtain the total number of platelets attached to each graft. To exclude the effect of BM-MNC number into BVGs, platelet numbers attached on BM-MNC-seeded BVGs were measured as the difference of absorbance between BM-MNC-seeded BVGs incubated into PRP and BM-MNC-seeded BVGs incubated into PBS, and are compared with those attached on unseeded BVGs.

2.5. Graft implantation

BM-MNC-seeded BVGs and unseeded BVGs were implanted into wild type C57BL/6 mice as inferior vena cava interposition conduits (n = 10, respectively). In addition, $c\text{-}Mpl^{-/-}$ and Pf4-Cre$^+$; iDTR mice were also implanted with unseeded BVGs using standard microsurgical technique by two micro surgeons (T.Y. and Y.L.) (n = 10, respectively) [8,10]. In brief, mice were anesthetized with intraperitoneal injections of ketamine (100 mg/kg), xylazine (10 mg/kg), and ketoprofen (5 mg/kg), a midline laparotomy incision was made, and the abdominal aorta was exposed. After transection of the inferior vena cava, a 3-mm graft was introduced with end-to-end anastomosis performed at both the proximal and distal ends using 10–0 monofilament nylon sutures in simple interrupted stitches. During implantation, grafts were flushed with a heparin solution (1000 U/ml, Fresenius Kabi USA, Lake Zurich, IL) to inhibit graft thrombosis. Following anastomosis, the surgical clamps were removed, and the abdomen was closed with a running 5-0 Prolene suture. Postoperatively, mice did not receive anticoagulation or antiplatelet therapy.

2.6. Ultrasound

Serial ultrasonography (Vevo Visualsonics 770; Visualsonics, Toronto, Ontario, Canada) was used to serially monitor grafts after implantation at 2, 4, and 8 weeks to determine patency. Before ultrasonography, mice were anesthetized with 1.5% v/v inhaled isoflurane. In this study, BVGs was defined as patent when venous flow was detected within the BVG, which was assessed by both color Doppler and pulse wave Doppler.

2.7. Histology and immunohistochemistry

All mice were sacrificed at 8 weeks. Explanted grafts were fixed in 4% paraformaldehyde, embedded in paraffin, and sectioned 5 μm thick. Sections were stained histologically with Carstair's Method (Rowley Biochemical Inc. Danvers, MA) to distinguish fibrin and platelets, von Willebrand factor antibody (Dako A0082, 1:1000, Agilent, Santa Clara, CA) for platelets, and Masson's Trichrome for collagen fibers. For immunofluorescence staining, endothelial cells were stained using rabbit anti-CD31 primary antibody (1:50, ab28364, Abcam, Cambridge, UK) and smooth muscle cells were stained using mouse anti-α-SMA primary antibody (1:500, Agilent). Secondary fluorochrome conjugated antibodies were Alexa Flour 488 anti-rabbit immunoglobulin G secondary antibody (1:300, Invitrogen, Carlsbad, CA) and Alexa Fluor 647 anti-mouse immunoglobulin G secondary antibody (1:300, Invitrogen), respectively. Images were obtained under a fluorescence microscope (Zeiss AXIO Observer Z1, Oberkochen, Germany).

2.8. Statistical analysis

Numeric values are listed as mean ± standard deviation. The number of experiments is shown in each case. For comparisons among multiple groups, data of continuous variables with normal distribution were evaluated by one-way ANOVA followed by Tukey–Kramer. A nonparametric Kruskal-Wallis test was used in instances when data had a non-normal distribution. A post hoc Mann–Whitney test was performed to detect significant differences between groups with Bonferroni-Holm correction for multiple comparisons, when the Kruskal-Wallis test was significant. Fisher's exact probability test was used for dichotomous variables of multiple groups. P values of <0.05 indicate statistical significance. All statistical analyses were performed using GraphPad Prism 7 (GraphPad Software, La Jolla, CA).

3. Results

3.1. Platelet numbers in platelet depletion models

To assess the effect of platelet number on graft patency, two mouse models were prepared (c-Mpl$^{-/-}$ and Pf4-Cre$^+$; iDTR). C-Mpl is the receptor for thrombopoietin, which is the main megakaryocyte (MK) growth factor. In c-Mpl knockout mice (*c-Mpl$^{-/-}$* mice), it has been well described that platelet numbers are reduced >85% relative to littermate controls [11]. In this study, platelet numbers were compared between c-Mpl$^{-/-}$ mice and C57BL/6 mice before graft implantation (day 0) and at explantation (day 56). Platelet number in c-Mpl$^{-/-}$ mice was significantly lower than in C57BL/6 mice at both time points (day 0; 147.4 ± 35.8 vs $503.8 \pm 111.0 \times 10^3/mm^3$, p = .012, and day 56; 139.2 ± 15.0 vs 497.2 ± 21.3, p < .001) (Fig. 1A), indicating chronic depletion of platelets in this model. In contrast, in Pf4-Cre$^+$; iDTR mice, platelets and MKs can be conditionally depleted by a Cre-recombinase-medicated cell ablation system. Upon diphtheria toxin (DT) exposure, platelet and MKs that are platelet factor 4 (Pf4)-positive cell populations, are susceptible to DT-induced apoptosis, leading to their systemic depletion. We administered DT intraperitoneally to Pf4-Cre$^+$; iDTR mice every other day for 2 weeks, and we observed the change of

platelet numbers with time. Platelet number decreased after DT injection, and depletion peaked at day 6 ($2.33 \pm 0.15 \times 10^5$/mm^3). The decrease in platelet number was sustained until day 14 at which time DT injection was ceased. After this time, platelet number increased and reached a plateau at day 18 (Fig. 1B).

3.2. Graft patency

BM-MNC-seeded BVGs and unseeded BVGs were implanted into wild type C57BL/6 mice as inferior vena cava interposition conduits (n = 10, respectively, Fig. 2A, B). To evaluate platelet effect on acute thrombosis, c-Mpl$^{-/-}$ and Pf4-Cre$^+$; iDTR mice were also implanted with unseeded BVGs (n = 10, respectively). Mice were followed by serial ultrasound at 2, 4, and 8 weeks after implantation (Fig. 2C, D). BM-MNC-seeded BVGs demonstrated a significantly higher patency rate during the acute phase (2-week) than unseeded BVGs (90% vs 30%, p = .020, Fig. 3A), and patency rates of these grafts were sustained until week 8 (90% vs 20%, p = .006, Fig. 3B). C-Mpl$^{-/-}$ and Pf4-Cre$^+$; iDTR mice also showed favorable graft patency (90% and 80%) during the acute phase (Fig. 3A). However, the patency rate of Pf4-Cre$^+$; iDTR mice decreased to 50% between the 2 to 4 week time points simultaneous to the recovery of platelet numbers (Fig. 3B). In these experiments, platelet number was associated with BVG patency, indicating that lower platelet number may inhibit platelet aggregation and thrombus formation during the acute phase after BVG implantation. There were no cases of aneurysmal formation or graft rupture, and all mice were sacrificed at 8 weeks.

3.3. Histomorphology

To elucidate the mechanism of acute BVG failure, unseeded BVGs were implanted into three C57BL/6 mice for 1 day and evaluated histologically; one remained patent and two became occluded. The patent BVG had a thin platelet-rich, or white thrombus, layer on the luminal surface of the BVG that occupied 10.9% of the lumen area (Fig. 4A, B, arrowheads). Of the two occluded BVG, one was assayed histologically to provide a rough characterization. The occluded BVG also possessed a white thrombus layer on its luminal surface of BVG (Fig. 4C, D, arrowheads) but was occluded by red thrombus that formed inside of the white thrombus layer (Fig. 4D-1 white arrowheads). Total thrombus area accounted for 96.8% of lumen area, and the proportion of white thrombus and red thrombus were 36.7 and 63.3%, respectively. Red thrombi contain red blood cells trapped within a fibrin network.

However, we could not distinguish fibrin in sections stained using Carstair's Method. This may be because the fibrin formed as thin fibers that are difficult to resolve interspersed within strongly stained and densely packed red blood cell. These findings suggest that platelet adhesion and aggregation on the luminal surface of BVGs might be a common phenomenon during the acute phase regardless of whether BVG remains patent or becomes completely occluded. At 8 weeks, occluded BVGs showed rich collagen and fewer smooth muscle cells than patent BVG (Fig. 4H-J). Collagen accounted for 24.6% of vessel area in patient BVGs, but 47.2% in occluded BVG, consistent with the high collagen content typically observed in organized thrombi [12,13].

In addition, to elucidate BVG characteristics at 8 weeks, histological sections were stained with hematoxylin and eosin and imaged using polarized light microscopy (Supplementary Fig. 1). These images revealed the disappearance of the scaffold by the 8-week time point. This finding is consistent with a previous in vivo study using a similar BVG also manufactured by Gunze Ltd. A BVG composed of PGA knitted fibers and a PLCL sponge lost half of its tensile strength in 2–3 weeks and all of it within 10 weeks [14]. Together, these data suggest that our BVG scaffold had mostly degraded at 8 weeks and lost most of its mechanical strength.

3.4. In vitro platelet attachment on BVGs

To characterize the effect of BM-MNC-seeding on platelet adhesion, BM-MNC-seeded BVGs and unseeded BVGs were incubated in platelet rich plasma in vitro and the number of attached platelets was quantified indirectly using an LDH assay. BM-MNC-seeding of BVGs significantly inhibited platelet adhesion compared to unseeded BVGs (1.75 ± 0.45 vs $8.69 \pm 0.68 \times 10^3$ platelet/mm^2, p < .001, Fig. 3C). Therefore, these data suggest that BM-MNC-seeding possibly encourages BVG patency by inhibiting platelet adhesion to the luminal surface of the scaffold.

4. Discussion

The present study demonstrates that BM-MNC-seeding improved BVG patency and suggests that it may also prevent acute BVG thrombosis. Based on a previous finding that antiplatelet drugs improved BVG patency during the early phase [6], we focused on the role of platelets in thrombus formation within BVGs.

For mice implanted with unseeded scaffolds, in two platelet reduction mouse models, the BVG patency rate was high relative to wild type mice. In the Pf4-Cre$^+$; iDTR mice, the patency rate decreased
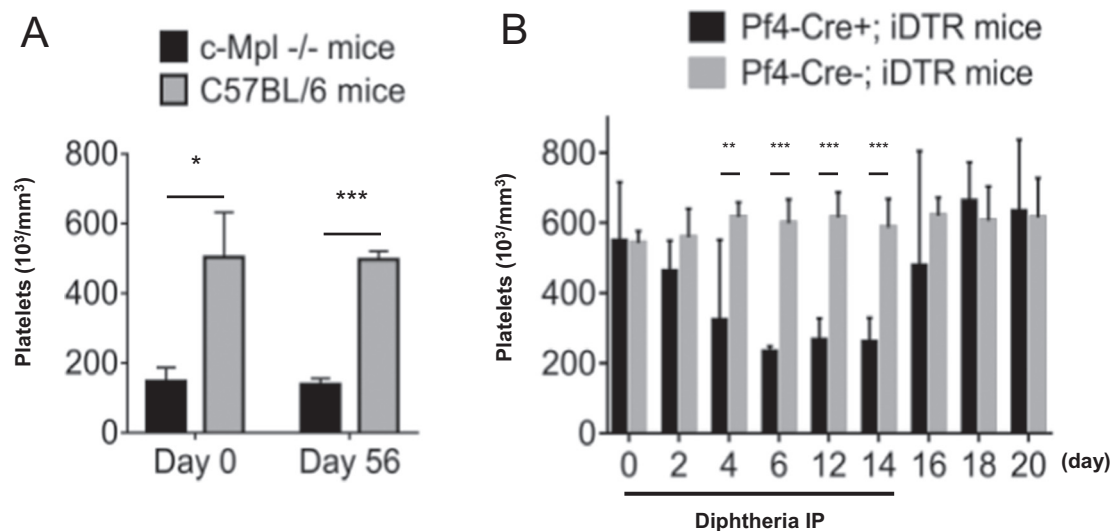

Fig. 1. Platelet numbers in platelet depletion mouse models. A, Platelet numbers in c-Mpl$^{-/-}$ and C57BL/6 mice before implantation and at explantation. B, Platelet number trends after diphtheria injection in Pf4-Cre$^+$; iDTR and Pf4-Cre$^-$; iDTR mice.
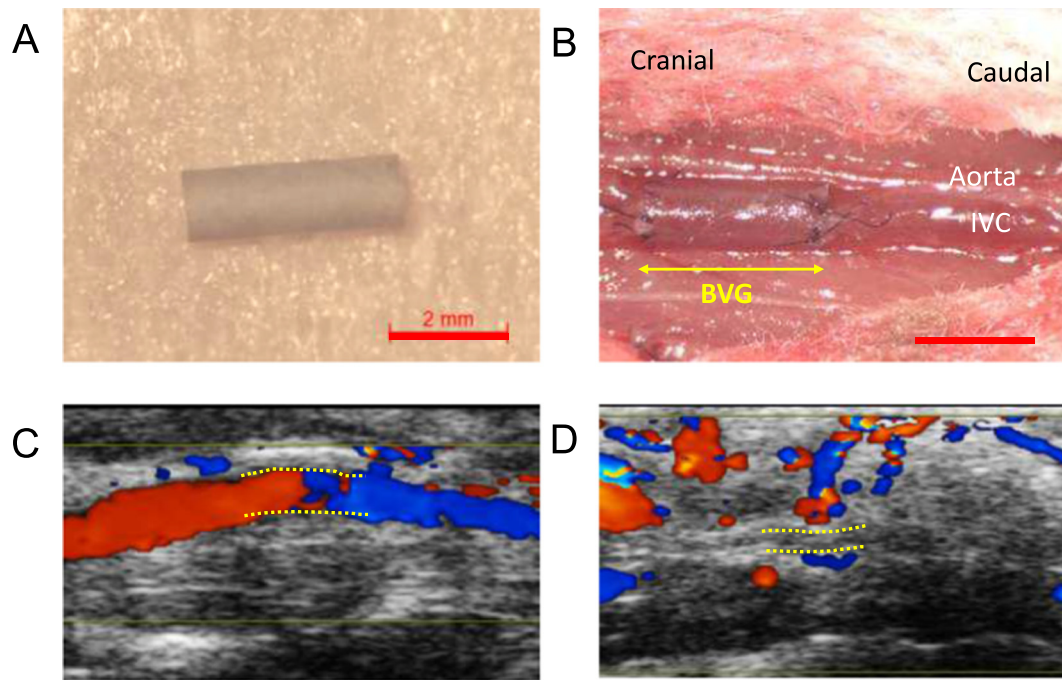
Fig. 2. Bioresorbable vascular graft implantation and ultrasound images. Macroscopic image of graft before implantation (A) and after implantation (B). Ultrasound images of grafts 8 weeks after implantation (C; patent, and D; occluded). Bar scale; 2 mm (A, B),

simultaneous to the recovery of platelet numbers. Histomorphological findings indicated platelets adhere on the luminal surface of BVGs during the early phase and occluded BVGs showed co-existence of white and red thrombi. Therefore, platelets appear to play a crucial rule in thrombus formation on BVGs during the early phase.

In addition, our in vitro study demonstrated that BM-MNC-seeding inhibited platelet adhesion on BVGs. Inflammatory cells including monocytes, macrophages, neutrophils, and B lymphocytes express the nucleotidases CD39 and CD73. These surface expressed enzymes degrade ATP and the platelet agonist ADP to AMP and adenosine,
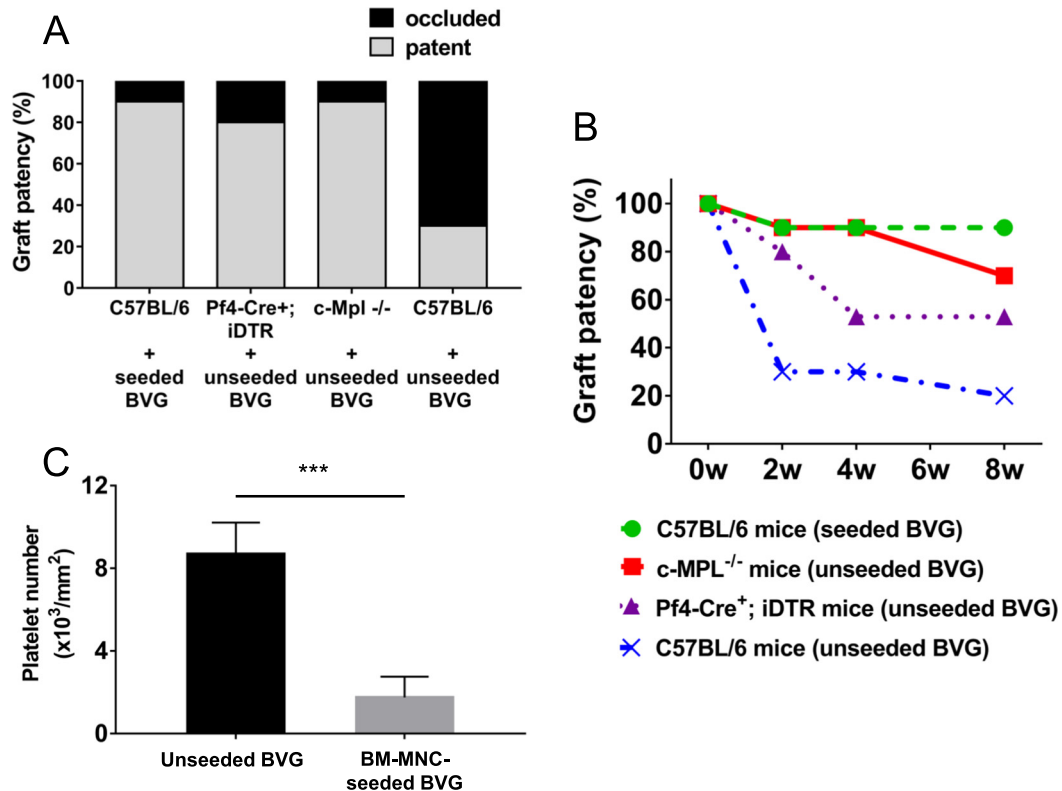

Fig. 3. BVG patency and platelet adhesion on BVGs in vitro. A, 2-week graft patency rate in all graft implantation models. The graft patency rate in C57BL/6 mice was 30%. However, the graft patency rates in other models were >80%. B, Serial graft patency rates in all graft implantation models by ultrasound findings. 8-week graft patency rates depended on 2-week graft patency except Pf4-cre+; iDTR mice. C, Platelet adhesion on BM-MNC-seeded BVGs and unseeded BVGs. BM-MNC-seeding inhibited platelet adhesion on BVGs. ***P < .001.
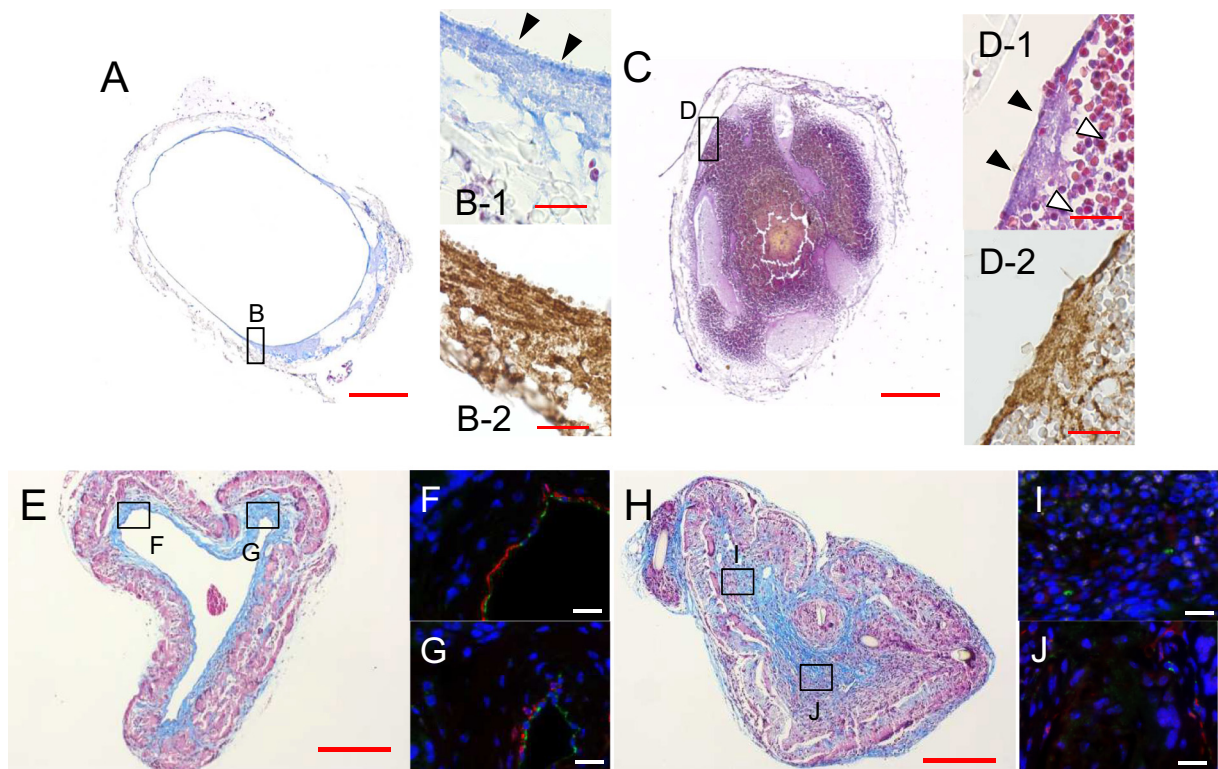
Fig. 4. Representative histomorphological findings of BVGs. At day 1 after BVG implantation, a patent BVG (A, B-1; Carstairs' Method, B-2; vWF antibody staining) showed a thin platelet-rich layer in the luminal side of BVG (B-1, arrowheads). An occluded BVG (C, D-1; Carstairs' staining, D-2; vWF antibody staining) showed platelet-rich layers (D-1, arrowheads) and a large red thrombus in the luminal side of BVG (D-1, white arrowheads). The microscopic findings of the neovessel at 8 weeks are shown at which time the BVG scaffold had largely degraded. A patent neovessel showed a thick collagen layer (E; Masson's Trichrome) and thin SMC layer (F, G; Immunofluorescent staining, Green; CD31, Red; α-SMA) in the luminal side. An occluded neovessel showed rich collagen and less SMCs (H–J). This finding was consistent with organized thrombi. Bar scale; 200 μm (A, C, E, H), 20 μm (B, D, F,G, I, J).

respectively, and have been shown to regulate platelet adhesion [15,16]. Thus, inflammatory cells in BM-MNCs possibly quench the prothrombotic signals and exert a protective antithrombotic effect. An alternative mechanism reported by Hashi et al. revealed the antithrombogenic property of bone marrow mesenchymal stem cells depended on cell-surface heparan sulfate proteoglycans that inhibited platelet adhesion [17]. We also previously revealed that BM-MNC-seeding attenuates platelet activation on BVGs [18], and, in a separate study, that reduced platelet activation by anti-platelet drug could improve the acute BVG patency [6]. Platelet adhesion and activation is a natural response to our scaffolds, a finding observed in both patent BVG and those that have become acutely thrombosed.

In our previous study, scanning electron microscope imaging of seeded BVG revealed the presence of BM-MNCs on the luminal surface [18]. However, a separate in vivo study showed that the number of BM-MNCs rapidly decreased after BVG implantation and were not detectable at 1 week [5]. Based on these previous findings and the results of the present study, we concluded that seeded BM-MNCs worked only in acute phase (within 1 week after implantation) with an anti-thrombotic effect.

In the present study, we demonstrated an anti-thrombotic effect of BM-MNCs by preventing platelet adhesion on a venous BVG. There findings may have broader implications for the prevention of thrombosis in intravascular devices including intra-arterial therapy, such as percutaneous coronary intervention (PCI) or transcatheter aortic valve replacement (TAVR). For example, in the field of PCI, a new bioabsorbable polymer stent composed of poly(L-lactic acid) (PLLA) is being evaluated clinically. Compared to the metallic stent, the bioresorbable vascular scaffold (BVS) was shown to be associated with a higher incidence of device thrombosis through 2-year follow-up, attributed at least in part

to the larger stent struts as they associated with blood-flow alternations and thrombogenicitiy [19]. However, the biodegradable polymer may also affect the thrombogenicity. Therefore, as a clinical implication for arterial BVGs, BM-MNC-seeding on BVGs may be a useful option to prevent acute BVG thrombosis. It is also worth considering BM-MNC-seeding for patients do not respond well to the established anti-platelet therapy due to bleeding complications, allergic response, or non-responsiveness to treatment.

4.1. Study limitations

Several limitations of this study should be noted. First, the precise mechanism of BM-MNC-seeding on BVG thrombosis remains to be fully elucidated in this study. As described above, several mechanisms have been suggested. However, further experiments will be needed. Second, other thrombogenic factors such as material property, surface structure, electrical charge, or fabrication were not evaluated in this study.

5. Conclusion

In this study, BM-MNC-seeding and the reduction in platelet number prevented BVG thrombosis and improved BVG patency. In addition, an in vitro study revealed BM-MNC-seeding inhibited platelet adhesion to the BVG. Based on these findings, we conclude that one possible effect of BM-MNC-seeding on BVG is inhibition of thrombus formation via platelet adhesion on BVGs.

Supplementary data to this article can be found online at https://doi.org/10.1016/j.ijcard.2018.01.059.

Sources of funding

Conflict of interest

Dr. Breuer is on the scientific advisory board for Cook Biomedical and is the founder of Lyst Therapeutics. Dr. Shinoka receives research support from Gunze Limited. The other authors report no conflicts of interest.

Acknowledgement

References

[1] T. Shin'oka, Y. Imai, Y. Ikada, Transplantation of a tissue-engineered pulmonary artery, N. Engl. J. Med. 344 (2001) 532–533.

[2] N. Hibino, E. McGillicuddy, G. Matsumura, Y. Ichihara, Y. Naito, C. Breuer, et al., Late-term results of tissue-engineered vascular grafts in humans, J Thorac Cardiovasc Surg. 139 (431-6) (2010) 6 e1-2.

[3] D.R. Duncan, P.Y. Chen, J.T. Patterson, Y.U. Lee, N. Hibino, M. Cleary, et al., TGFbetaR1 inhibition blocks the formation of stenosis in tissue-engineered vascular grafts, J. Am. Coll. Cardiol. 65 (2015) 512–514.

[4] N. Hibino, T. Yi, D.R. Duncan, A. Rathore, E. Dean, Y. Naito, et al., A critical role for macrophages in neovessel formation and the development of stenosis in tissue-engineered vascular grafts, FASEB J. 25 (2011) 4253–4263.

[5] J.D. Roh, R. Sawh-Martinez, M.P. Brennan, S.M. Jay, L. Devine, D.A. Rao, et al., Tissue-engineered vascular grafts transform into mature blood vessels via an inflammation-mediated process of vascular remodeling, Proc. Natl. Acad. Sci. U. S. A. 107 (2010) 4669–4674.

[6] Y.U. Lee, Ruiz-Rosado J. de Dios, N. Mahler, C.A. Best, S. Tara, T. Yi, et al., TGF-beta receptor 1 inhibition prevents stenosis of tissue-engineered vascular grafts by educing host mononuclear phagocyte activation, FASEB J. 30 (2016) 2627–2636.

[7] J.D. Roh, G.N. Nelson, M.P. Brennan, T.L. Mirensky, T. Yi, T.F. Hazlett, et al., Small-diameter biodegradable scaffolds for functional vascular tissue engineering in the mouse model, Biomaterials 29 (2008) 1454–1463.

[8] Y.U. Lee, T. Yi, S. Tara, A.Y. Lee, N. Hibino, T. Shinoka, et al., Implantation of inferior vena cava interposition graft in mouse model, J. Vis. Exp. 88 (2014), e51632. .

[9] S. Tara, H. Kurobe, J. de Dios Ruiz Rosado, C.A. Best, T. Shoji, N. Mahler, et al., Cilostazol, not aspirin, prevents stenosis of bioresorbable vascular grafts in a venous model, Arterioscler. Thromb. Vasc. Biol. 35 (2015) 2003–2010.

[10] T.L. Mirensky, G.N. Nelson, M.P. Brennan, J.D. Roh, N. Hibino, T. Yi, et al., Tissue-engineered arterial grafts: long-term results after implantation in a small animal model, J. Pediatr. Surg. 44 (2009) 1127–1132 (discussion 32-3).

[11] A.L. Gurney, K. Carver-Moore, F.J. de Sauvage, M.W. Moore, Thrombocytopenia in c-mpl-deficient mice, Science 265 (1994) 1445–1447.

[12] K. Sakakura, M. Nakano, F. Otsuka, K. Yahagi, R. Kutys, E. Ladich, et al., Comparison of pathology of chronic total occlusion with and without coronary artery bypass graft, Eur. Heart J. 35 (2014) 1683–1693.

[13] H. Mori, C. Lutter, K. Yahagi, E. Harari, R. Kutys, D.R. Fowler, et al., Pathology of chronic total occlusion in bare-metal versus drug-eluting stents, Implications for Revascularization. JACC Cardiovasc Interv. 10 (2017) 367–378.

[14] G. Matsumura, N. Nitta, S. Matsuda, Y. Sakamoto, N. Isayama, K. Yamazaki, et al., Long-term results of cell-free biodegradable scaffolds for in situ tissue-engineering vasculature: in a canine inferior vena cava model, PLoS One 7 (2012), e35760.

[15] R. Covarrubias, E. Chepurko, A. Reynolds, Z.M. Huttinger, R. Huttinger, K. Stanfill, et al., Role of the CD39/CD73 purinergic pathway in modulating arterial thrombosis in mice, Arterioscler. Thromb. Vasc. Biol. 36 (2016) 1809–1820.

[16] Y.M. Kanthi, N.R. Sutton, D.J. Pinsky, CD39: interface between vascular thrombosis and inflammation, Curr Atheroscler Rep 16 (2014) 425.

[17] C.K. Hashi, Y. Zhu, G.Y. Yang, W.L. Young, B.S. Hsiao, K. Wang, et al., Antithrombogenic property of bone marrow mesenchymal stem cells in nanofibrous vascular grafts, Proc. Natl. Acad. Sci. U. S. A. 104 (2007) 11915–11920.

[18] T. Fukunishi, C.A. Best, C.S. Ong, T. Groehl, J. Reinhardt, T. Yi, et al., Role of bone marrow mononuclear cell seeding for nanofiber vascular grafts, Tissue Eng Part A. 24 (2017) 135–144.

[19] J.J. Wykrzykowska, R.P. Kraak, S.H. Hofma, R.J. van der Schaaf, E.K. Arkenbout, I.J. AJ, et al., Bioresorbable scaffolds versus metallic stents in routine PCI, N. Engl. J. Med. 376 (2017) 2319–2328.